DE GRUYTER
OPEN

Contributions to Geophysics and Geodesy Vol. 44/2, 2014 (133–147)

Determination of shear surface of landslides using electrical resistivity tomography

Ivan DOSTÁL, René PUTIŠKA, David KUŠNIRÁK

Department of Applied and Environmental Geophysics, Faculty of Natural Sciences
Comenius University, Mlynská dolina, pav. G, 842 48 Bratislava, Slovak Republic
e-mail: dostal@fns.uniba.sk, putiska@fns.uniba.sk, kusnirak@fns.uniba.sk

Abstract: Geophysical methods offer a broad spectrum of information by dealing with slope deformations. The electrical resistivity tomography (ERT) method is mainly applied for spatial localization of the landslide body and depicting the shear zone position. This article presents the application of the ERT method for the landslide hazardous areas by means of numerical modelling. Four different synthetic models with very small resistivity contrast (30 Ohm.m/50 Ohm.m), where each model represents a different type of slope deformation, were tested by several factors affecting the final inverse model: measurement point density, L_1 and L_2 norm and L-norm roughness filter components. The higher measurement points density helps mainly to detect the boundaries at greater depths. Inverse models computed using the L_1 norm bring satisfactory results for compact anomalous bodies, i.e. water saturated landslide body. In the case of subtle conductive zones, i.e. shear planes, the L_2 norm based inversion is recommended. For enhanced reconstruction of skewed anomalous objects, roughness filter including a diagonal component produces more accurate inverse image. The article also demonstrates the ability of the ERT method to detect and describe the shape of the slope deformation even by a relative subtle resistivity contrast.

Key words: applied geophysics, electrical resistivity tomography, resistivity modelling, resistivity inversion, landslides

1. Introduction

Slope deformations arise by a decrease of shear parameters of rocks and soils, where the landslide body is divided to form the intact surroundings by shear surface along which a movement has occurred. The exact shear surface localization is an essential information for engineering geologist not

doi: 10.2478/congeo-2014-0008

even for stability assessment of the hazardous area, but also for modelling of spatial distributions of various slope-deformation forms (*Holec et al., 2013*). Currently, the electrical resistivity tomography (ERT), as well as other geophysical methods, are widely used in the slope deformations evaluation and prediction (*Bednárik et al., 2010; Constantin et al., 2011; Bekler et al., 2011; Socco et al., 2010; Tric et al., 2010*). The most common application of the ERT method is to locate the body of the landslide in the studied area (*Jomard et al., 2010; Pánek et al., 2008*).

A landslide shear zone is often formed by rocks that are becoming unstable after their saturation with water, i.e. clay materials. Such material should be identified in the resistivity field as conductive anomaly, so ERT method should be able to identify the described kind of anomaly. Crucial factors in determining such objects are: density of measurement points, effective depth, sensitivity and resolution of the chosen electrode array. The density of data points is directly dependent on the chosen electrode distance (*Dahlin and Zhou, 2004*). Effective depth of the survey depends on the total length of multi-electrode system and electrodes arrangement (*Edwards, 1977*). The sensitivity and resolution of any electrode array is directly dependent on the position of potential and current electrodes (*Loke, 2014; Zhou et al., 2002*).

In this paper we present the results of synthetic modeling realized on the four different idealized landslides models. The influence of the L_1 and L_2 norms on the inverse problem calculation is examined, and the resulting change in the inverse resistivity models are described and cross-checked with the input models. We tested the effect of measuring points density using two electrode distances for the electrode arrangement dipole-dipole, which is suitable array for detection of isometric structures (*Putiška et al., 2012a; Putiška et al., 2012b; Dahlin and Zhou, 2004*). The main objective of the proposed synthetic test was to point out the peculiarities that arise from the application of the ERT method to landslide areas.

2. Synthetic test

Since landslides occur mainly in environments consisting of clay or clay-sandy sediments (*Bievre et al., 2012*), and in the Neogene and Paleogene

rock environments, we focused on this problem during the creation of synthetic models. We designed four landslide scenarios with very low resistivity contrast between the landslide body (30 Ohm.m) and the host rock (50 Ohm.m). Each model has surface layer with a thickness of 0.5 m and a resistivity value of 100 Ohm.m, which approximates the Quaternary clay layer.

Model #1 (Fig. 2a) represents a shape of the landslide body with a small thickness (5.0 m) and planar shear surface.

Model #2 (Fig. 3a) approximates the shape of the landslide body of greater thickness (max 12.0 m) and quasi-cylindrical shear surface.

Model #3 (Fig. 4a) represents a relatively thin shear zone (about 2.0 m) of a quasi-cylindrical shape surrounded by a homogeneous medium.

Model #4 (Fig. 5a) is designed as a complex shear zone shape (combination of the cylindrical and planar shear zone).

2.1 Forward modelling

The forward modeling tool allows us to simulate a field measurement by the selected electrode array and obtain a synthetic dataset of apparent resistivity values. The Res2DMod modeling software (*Loke and Barker, 1996*) has been used for forward calculation, zero level of Gaussian noise was added into the final dataset.

All models consist of isometric bodies, so the dipole-dipole array (Fig. 1a) was selected as an optimal electrode array for the forward calculation. (*Putiška et al., 2012a; Putiška et al., 2012b; Dahlin and Zhou, 2004*).

To test the effect of density measurement points on the shape of the resistive bodies in the inverse crosssection for each model, we used a two-electrode distance (5.0 and 2.5 m) on the profile with a total length of 115.0 m (Fig. 1). The forward calculation of the apparent resistivity values is governed by the parameters a (minimal electrode spacing) and n (separation factor) of the dipole-dipole electrode array. For our test, the following parameters were used: $a = 5 - 15$ m, $n = 1 - 6$ (for an electrode distance of 5.0 m), and the parameters $a = 2.5 - 25$ m, $n = 1 - 6$ (for an electrode distance of 2.5 m). The total number of points calculated into datasets for an electrode distance of 5.0 m and 2.5 m were 374 and 1894 apparent resistivity values respectively (Figs. 1b, 1c).

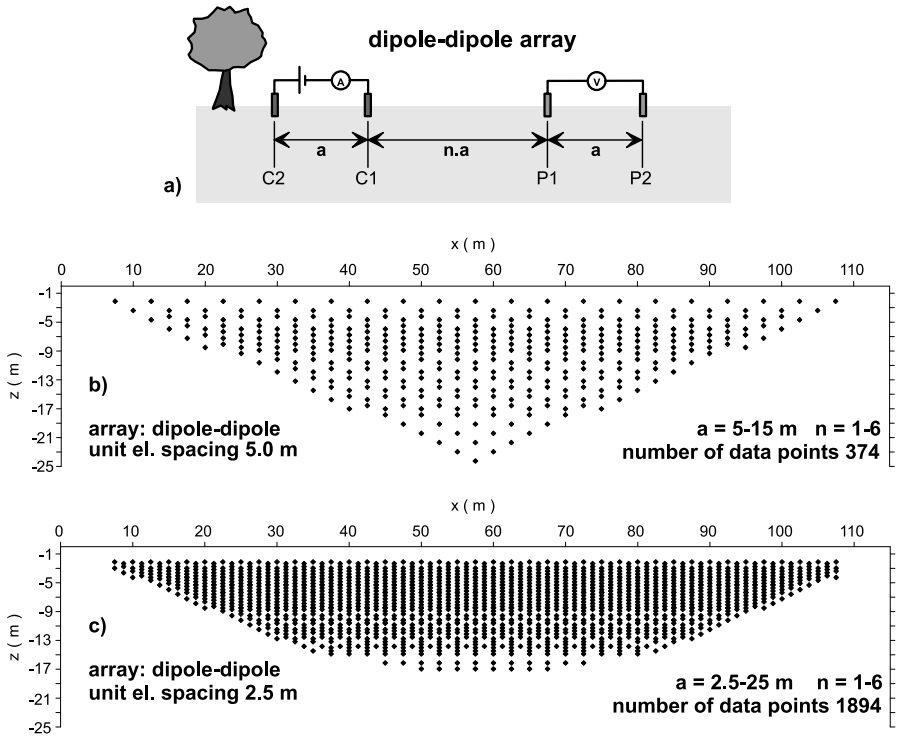

Fig. 1. a) sketch of dipole-dipole array; b) number of data point used in forward modelling for electrode spacing 5.0 m; c) number of data point used in forward modelling for electrode spacing 2.5 m.

As the landslides occur almost exclusively on the slopes, in Slovakia most affected slopes are within the range 7 to 12 degrees (*Bednárik and Liščák, 2009*), a fictious uniform topography was considered in the models, defined as $z = 300$ m for $x = 0$ m and $z = 290$ m to $x = 115$ m.

2.2 Inverse modelling

Since the measured data (apparent resistivity) do not provide desired information about the subsurface resistivity distribution directly, inversion technique has to be employed to reconstruct the actual distribution. For the inverse calculation of the synthetic datasets the Res2DInv (*Loke and*

Barker, 1996) was used. Standard roughness vertical and horizontal filters were applied for the inversion calculation utilizing L_1 a L_2 for the evaluation of a governing functional.

The L_2 norm inversion method gives optimal results where subsurface geology exhibits a smooth variation, such as the diffusion boundary of a chemical plume. However, in cases where the subsurface consists of bodies that are internally homogeneous with sharp boundaries (such as an igneous dyke) this method tends to smooth out the boundaries. The L_1 norm or blocky optimization method tends to produce models that are piecewise constant (*Ellis and Oldenburg, 1994*).

For the synthetic datasets produced from electrode distance 5.0 m and 2.5 m inverse models consisting of 31 layers (726 model cells) and 41 layers (2492 model cells) were used, respectively. Main inversion parameters and settings are summarized in the Table 1.

Table 1. Main inversion parameters used for the calculation for all presented inverse models

Inversion Parameter	**Value**
number of iterations	7
initial damping factor	0.15
increase of damping factor with depth	1.05
vertical to horizontal flatness filter ratio	1
thickness of first layer	0.3
factor to increase thickness layer with depth	1.01
model refinement	half width cells
type of reference model	average resistivity
damping factor for reference model	0.01
forward modelling numerical approach	finite element method

3. Test results

Model #1

Synthetic model #1 was chosen as a simple type of landslide body with planar shear surface (Fig. 2a). Evident resistivity anomaly is present on all

inverse sections, which is produced by the slightly less resistive modelled landslide body 30 Ohm.m than the stable bedrock (50 Ohm.m). Differences in the application of the standard L_1 (Figs. 2b, 2d) and L_2 norms (Figs. 2c, 2e) are only in the bottom border of the conductive body, arising from the mathematical principles of the involved norms. In the calculated inverse cross-sections for electrode distance of 5.0 m the uppermost thin subsurface layer is not reconstructed, as the measurement points do not cover this layer (Figs. 2b, 2c). For the case of the electrode distance 2.5 m, the thin subsurface layer is visible, but only in the area outside of the conductive body (Figs. 2d, 2e).

Model #2

Synthetic model #2 represents a conductive landslide body with cylindrical shear zone (Fig. 3a). For the case of electrode distance of 5.0 m the shape of the landslide body clearly visible in the inverse image, as well as the influence of the employed norm on the resolution of the bottom boundary (Figs. 3b, 3c). For the case of electrode distance of 2.5 m the inverse process was not able to reconstruct reliably the dipping shape of the shear zone (Figs. 3d, 3e), which is the effect of improper setting of the roughness filter. For this model the best results were obtained using the 5.0 m electrode distance and inverse calculation based on L_1 norm.

Model #3

Synthetic model #3 was created as an approximation of a relatively thin conductive shear zone in a homogenous environment (Fig. 4a). In the inverse models for electrode spacing 5.0 m (Figs. 4b, 4c) the conductive zone is significantly thicker than in the input models, as a consequence of lower measurement points density and equality of the inverse and model resistivity were achieved in the near surface areas only. The conductivity zone thickness fits very well in the inverse models with electrode spacing 2.5 m (Figs. 4d, 4e), thanks to higher density of the measurement points. The inverse model with use of L_2 norm (Fig. 4e) gives even a better result, where the conductive zone is better defined and the resistivity values are more approaching those which were modeled.

Model #4

Synthetic model #4 represents composite shape of two cylindrical shear

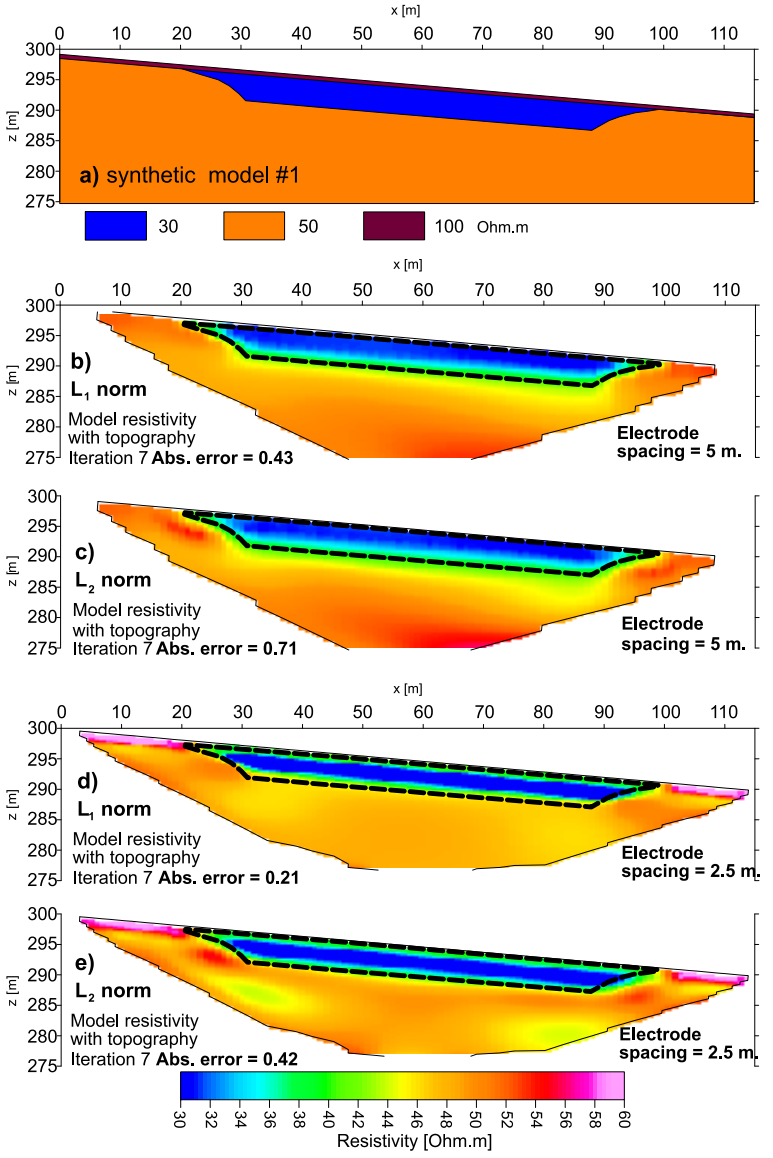

Fig. 2. Inverse model resistivity sections from synthetic data set: a) geometry of the synthetic model #1; b) inverse model with electrode spacing 5.0 m using the L_1 norm c) inverse model with electrode spacing 5.0 m using the L_2 norm; d) inverse model with electrode spacing 2.5 m using the L_1 norm e) inverse model with electrode spacing 2.5 m using the L_2 norm.

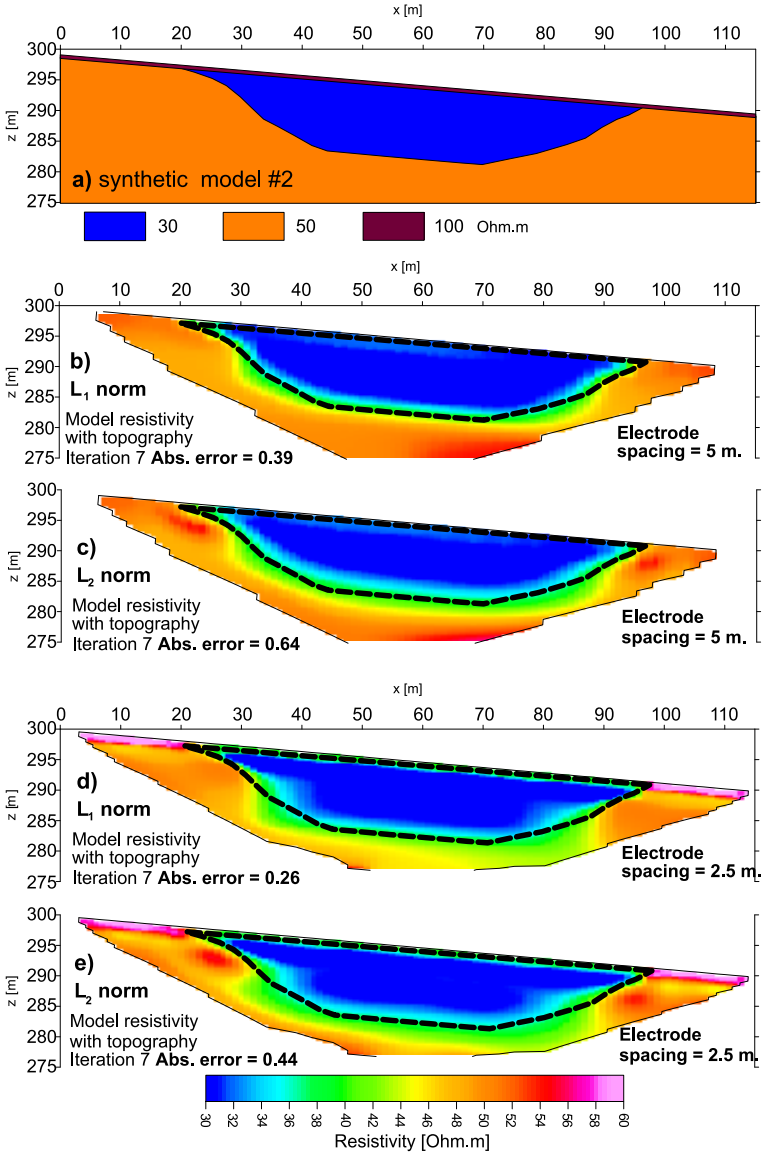

Fig. 3. Inverse model resistivity sections from synthetic data set: a) geometry of the synthetic model #2; b) inverse model with electrode spacing 5.0 m using the L_1 norm c) inverse model with electrode spacing 5.0 m using the L_2 norm; d) inverse model with electrode spacing 2.5 m using the L_1 norm e) inverse model with electrode spacing 2.5 m using the L_2 norm.

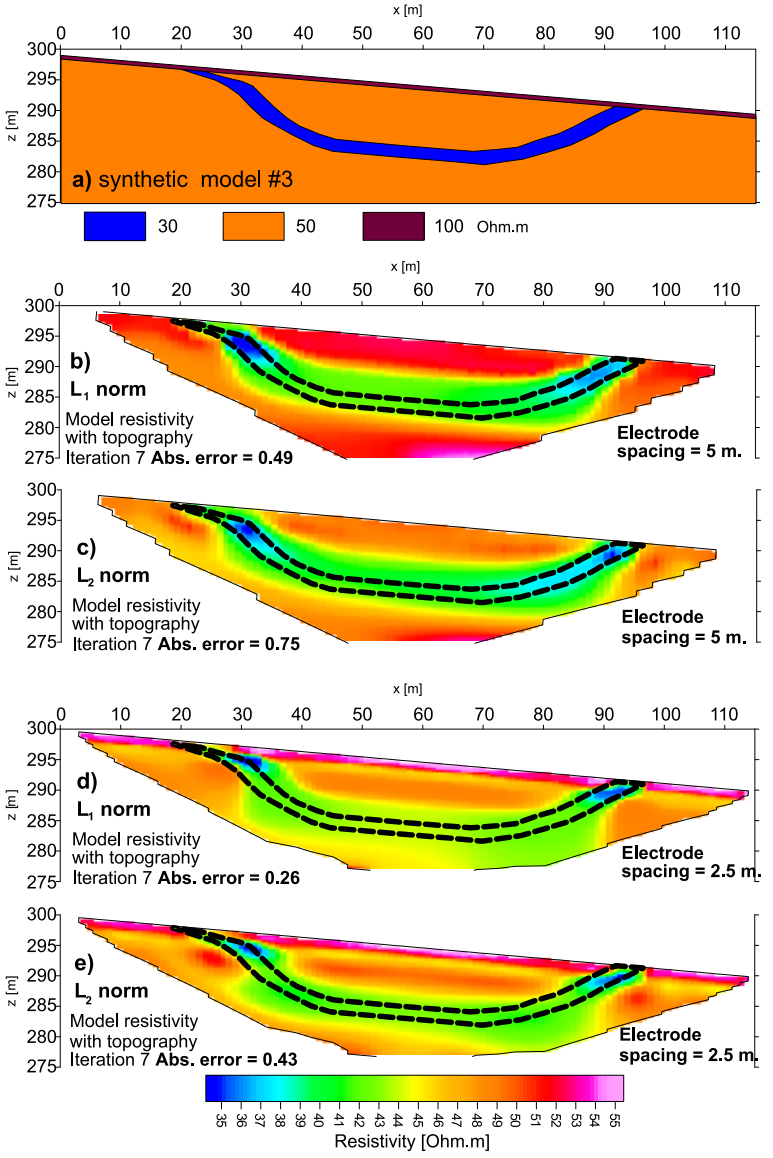

Fig. 4. Inverse model resistivity sections from synthetic data set: a) geometry of the synthetic model #3; b) inverse model with electrode spacing 5.0 m using the L_1 norm c) inverse model with electrode spacing 5.0 m using the L_2 norm; d) inverse model with electrode spacing 2.5 m using the L_1 norm e) inverse model with electrode spacing 2.5 m using the L_2 norm.

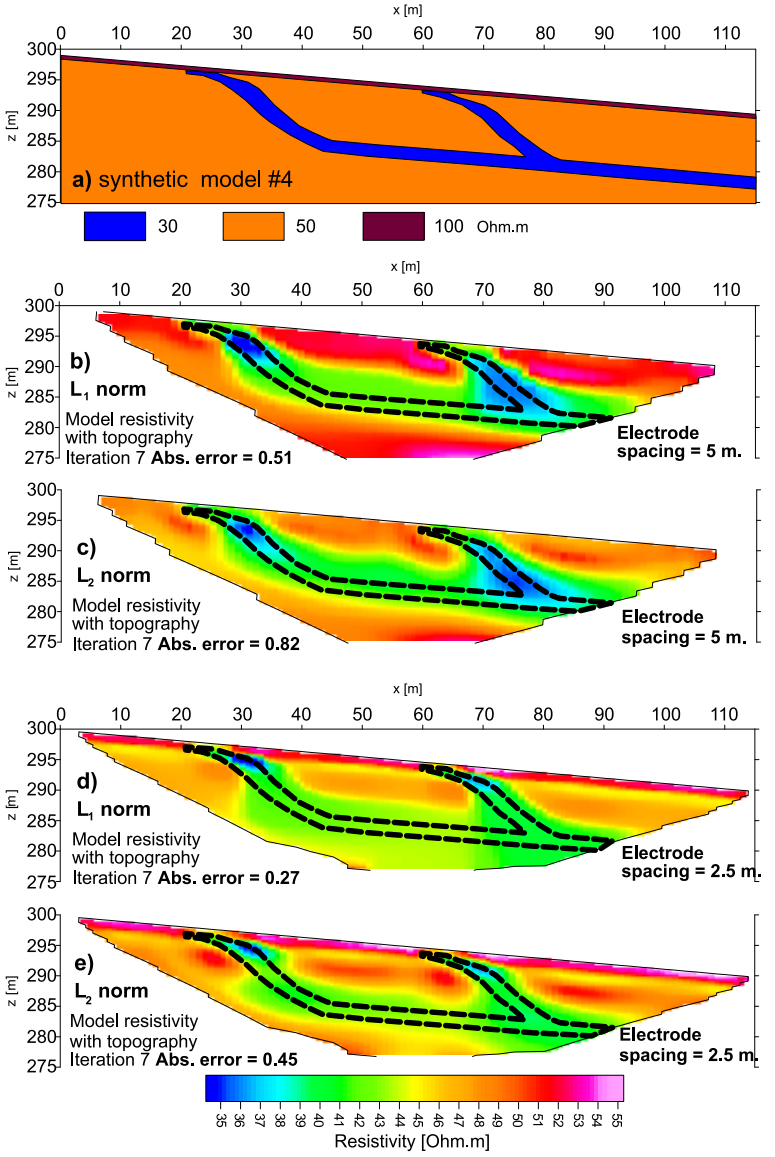

Fig. 5. Inverse model resistivity sections from synthetic data set: a) geometry of the synthetic model #4; b) inverse model with electrode spacing 5.0 m using the L_1 norm c) inverse model with electrode spacing 5.0 m using the L_2 norm; d) inverse model with electrode spacing 2.5 m using the L_1 norm e) inverse model with electrode spacing 2.5 m using the L_2 norm.

zones, which are joining into a planar shear zone (Fig. 5a). For both L norms the inverse models with electrode spacing 5.0 m (Figs. 5b, 5c) look basically the same. The shear zone is much thicker than it was modeled and the resistivity values are close to the modeled just in the thicker parts of the conductivity zones, because of lower measurement points density. The inverse models with electrode spacing 2.5 m (Figs. 5d, 5e) are in a good correlation with the modeled situation in the near surface parts (approximately the first 5 m). In the dipping conductivity zone area (in depth of 5–10 m) is visible the strong effect of the roughness filter to the inverse process again. The bottom parts of the inverse cross-section have different results for L_1 and L_2 norms. For inverse model with L_1 norm (Fig. 5d) the planar part of the shear zone is poorly bounded. A better result can be observed in the inverse model with L_2 norm (Fig. 5e), where the shear zone shape agrees well with the input model.

From results of all four synthetic models a major effect caused by vertical and horizontal L-norm roughness filters arises, where the modeled shear zone shape is not correctly reconstructed by means of least-square inversion. Therefore we involved, in addition to the standard vertical and horizontal roughness filter components, a diagonal filter component as well. Recomputed results for electrode spacing 2.5 m using the L_1 norm are shown in Fig. 6. In the case of model #1 (Fig. 6a) the improvement of the inverse model using the enhanced roughness filter is marginal, as the original result (Fig. 2d) provided very satisfactory inverse model. The change in the case of model #2 (Fig. 6b) is more significant as the inverse image of the subsurface depict more accurately the dipping edges of the shear zone and suppress the presence of artificial steps produced in the original result (Fig. 3d). Similar improvement is evident for the models #3 and #4, where the inversion using the diagonal filter reconstructs the lower boundary of the anomalous body better (Figs. 6c, 6d) comparing to the original results (Figs. 4d, 5d).

4. Conclusions

The ERT method is mostly used for location of the landslide body itself and for detection of the shear zone (surface) shape and extensions.The aim

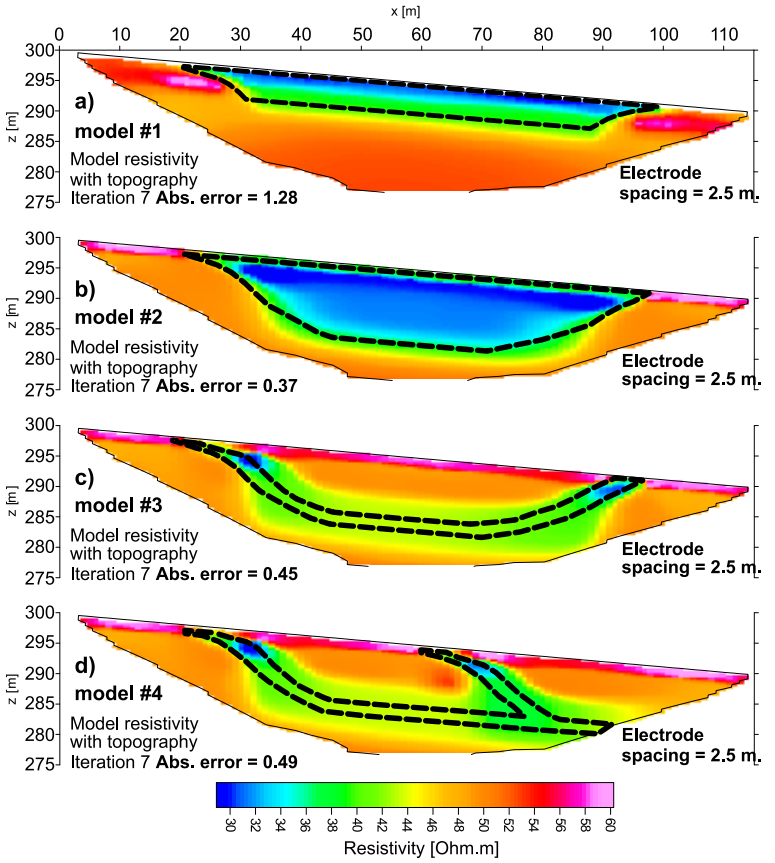

Fig. 6. Inverse model resistivity sections from synthetic data sets recomputed with enhanced filter by diagonal component using the L_1 norm. a) inversion results for model #1; b) inversion results for model #2; c) inversion results for model #3; d) inversion results for model #4.

of this paper was to point out the particularities which arise in the interpretation of ERT results in landslide areas. We have tested the influence of the measurement points density on the modeled bodies shape in the inverse cross-sections for dipole-dipole electrode array, as well as the influence of the L norms in the inversion calculation. Four synthetic models with challenging resistivity contrasts between modeled bodies (30 Ohm.m/50 Ohm.m) were utilized for this purpose.

From the synthetic modeling results, we found out that the higher measurement points density (especially in greater depths) expressively influences elementary shaped conductive bodies bottom boundary determination. The measurement points density is also an important attribute for thin conductive bodies detection. These situations occur in areas with slope deformations, where the shear zone has a minor thickness and is reaching greater depths.

In cases when the entire landslide body is formed by relatively homogenous material (model #1 and #2), inverse results employing L_1 norm are showing better correlation with the model situation (resistivity boundaries are sharp). In situations, when the landslide environment is formed by the same material but the present shear zone is thin (with lower resistivity than the entourage, model #3 and #4), better results offer the use of L_2 norm for the inverse calculation. A considerable influence on the inversion result has in such case also the applied smoothing filter. As it can be seen on inverse models #3 and #4 (Figs. 4d, 4e, 5d and 5e), used roughness filter is generating drop-structures (steps) on inclined interfaces. Therefore it's appropriate to use also a diagonal filter, which can improve the inversion results noticeable (Fig. 6). A significant improvement is observable for models containing bodies with skewed shape (Figs. 6b, 6c, 6d).

From the modeling results we state, that the ERT method is a suitable application for slope deformation survey, where the landslide body or shear zone has a relatively small resistivity contrast compared to the surrounding environment. Important influence on the inverse result can have a higher value of noise in the measured data. Therefore it's necessary to avoid methodical errors. Coincidental errors can be minimized by repeated measurements.

Acknowledgments. The authors are grateful to the Slovak Research and Development Agency APVV (grant nos. APVV-0129-12, APVV-0625-11, APVV-0724-11) and the Slovak Grant Agency VEGA (grant nos. 1/0131/14, 2/0067/12 and 1/0095/12) for the support of their research. This publication is the result of the project implementation: Comenius University in Bratislava Science Park supported by the Research and Development Operational Programme funded by the ERDF Grant number: ITMS 26240220086.

References

Bednárik M., Liščák P., 2009: Landslide susceptibility assessment in Slovakia. Mineralia Slovaca, **42**, 193–204.

Bednárik M., Magulová B., Matys M., Marschalko M., 2010: Landslide susceptibility assessment of the Kraľovany–Liptovský Mikuláš railway case study. Physics and Chemistry of the Earth, **35**, 3–5.

Bekler T., Ekinci Y. L., Demirci A., Erginal A. E., Ertekin C., 2011: Characterization of a landslide using seismic refraction, electrical resistivity and hydrometer methods, Adatepe–Canakkale, NW Turkey. Journal of Environmental and Engineering Geophysics, **16**, 115–126.

Bievre G., Jongmans D., Winiarski T., Zumbo V., 2012: Application of geophysical measurements for assessing the role of fissures in water infiltration within a clay landslide (Trieves area, French Alps). Hydrological Processes, **26**, 2128–2142.

Constantin M., Bednárik M., Jurchescu M. C., Vlaicu M., 2011: Landslide susceptibility assessment using the bivariate statistical analysis and the index of entropy in the Sibiciu Basin (Romania). Environmental Earth Sciences, **63**, 397–406.

Dahlin T., Zhou B., 2004: A numerical comparison of 2D resistiviy imaging with 10 electrode arrays. Geophysical Prospecting, **52**, 379–398.

Edwards L. S., 1977: A modified pseudosection for resistivity and induced-polarization. Geophysics, **42**, 1020–1036.

Ellis R. G., Oldenburg D. W., 1994: Applied geophysical inversion. Geophysical Journal International, **116**, 5–11.

Holec J., Bednárik M., Šabo M., Minár J., Yilmaz I., Marschalko M., 2013: A small-scale landslide susceptibility assessment for the territory of Western Carpathians. Natural Hazards, **69**, 1081–1107.

Jomard H., Lebourg T., Guglielmi Y., Tric E., 2010: Electrical imaging of sliding geometry and fluids associated with a deep seated landslide (La Clapiere, France). Earth Surface Processes and Landforms, **35**, 588–599.

Loke M. H., 2014: Rapid 2D resistivity inversion using the least-squares method. Res2DInv program manual, Penang, Malaysia, 180 p.

Loke M. H., Barker R. D., 1996: Rapid least-squares inversion of apparent resistivity pseudosections using a quasi-Newton method. Geophysical Prospecting, **44**, 131–152.

Pánek T., Hradecký J., Šilhán K., 2008: Application of electrical resistivity tomography (ERT) in the study of various types of slope deformations in anisotropic bedrock: case studies from the flysch Carpatians. Studia Geomorphologica Carpatho-Balcanica, **42**, 57–73.

Putiška R., Dostál I., Kušnirák D., 2012: Determination of dipping contacts using electrical resistivity tomography. Contrib. Geophys. Geod., **42**, 2, 161–180.

Putiška R., Nikolaj M., Dostál I., Kušnirák D., 2012b: Determination of cavities using electrical resistivity tomography. Contributions to Geophysics and Geodesy, **42**, 2, 201–211.

Socco L. V., Jongmans D., Boiero D., Stocco S., Maraschini M., Tokeshi K., Hantz D., 2010: Geophysical investigation of the Sandalp rock avalanche deposits. Journal of Applied Geophysics, **70**, 277–291.

Tric E., Lebourg T., Jomard H., Le Cossec J., 2010: Study of large-scale deformation induced by gravity on the La Clapiere landslide (Saint-Etienne de Tinee, France) using numerical and geophysical approaches. Journal of Applied Geophysics, **70**, 206–215.

Zhou W., Beck B. F., Adams A. L., 2002: Effective electrode array in mapping karst hazards in electrical resistivity tomography. Environmental Geology, **42**, 922–928.